

# AN EFFICIENT IMPLEMENTATION OF POWER MANAGEMENT IN PV-BATTERY-HYDRO BASED STANDALONE MICRO GRID

<sup>1</sup>B.MANI, <sup>2</sup>P.HEMANTH PRITHVI

<sup>1</sup>M.Tech Student, <sup>2</sup>Assistant Professor,

Department of EEE,

KAKINADA INSTITUTE OF TECHNOLOGICAL SCIENCES (KITS), RAMACHANDRAPURAM.

**Abstract:** This work deals with the frequency regulation, voltage regulation, power management and load levelling of solar photovoltaic (PV)-battery-hydro based microgrid (MG). In this MG, the battery capacity is reduced as compared to a system, where the battery is directly connected to the DC bus of the voltage source converter (VSC). A bidirectional DC-DC converter connects the battery to the DC bus and it controls the charging and discharging current of the battery. It also regulates the DC bus voltage of VSC, frequency and voltage of MG. The proposed system manages the power flow of different sources like hydro and solar PV array. However, the load levelling is managed through the battery. The battery with VSC absorbs the sudden load changes, resulting in rapid regulation of DC link voltage, frequency and voltage of MG. Therefore, the system voltage and frequency regulation allows the active power balance along with the auxiliary services such as reactive power support, source current harmonics mitigation and voltage harmonics reduction at the point of common interconnection. The experimental results under various steady state and dynamic conditions, exhibit the excellent performance of the proposed system and validate the design and control of proposed MG.

**Index Terms**—Solar PV System, Battery, Control and Power Management System, Distributed Energy Resource, Microgrid, Power Electronics.

## 1.INTRODUCTION

Continually increasing demand for energy and concerns of environmental deterioration have been spurring electric power experts to find sustainable methods of power generation. Distributed generations (DG) in the form of renewable resources, such as solar energy, are believed to provide an effective solution to reduce the dependency on conventional power generation and to enhance the reliability and quality of power systems. Photovoltaic (PV) power systems have become one of the most promising renewable generation technologies because of their attractive characteristics such as abundance of solar and clean energy. Rapid PV technology development and declining installation costs are also stimulating the increasing deployment of PV in power systems. However, due to the nature of solar energy and PV panels, instantaneous power output of a PV system depends largely on its operating environment, such as solar irradiance and surrounding temperature, resulting in constant fluctuations in the output power. Therefore, to maintain a reliable output power, battery storage systems are usually integrated with PV systems to address the variability issue.

A typical configuration of PV-battery system is illustrated in Fig. 1, which is a hybrid microgrid system consisting of a PV array that contains a number of PV panels, battery bank for power storage, and a centralized bidirectional inverter that interfaces the DC to AC power system. A unidirectional

DC/DC converter is installed to control the power of PV arrays, while the battery bank is charged/discharged by controlling a bidirectional converter that bridges the battery and the DC bus. DC loads are supplied through direct connection to the DC bus and AC loads and the point of common coupling (PCC) is located on the AC side. Before connecting to the utility grid, a transformer is employed to step up the AC voltage to that of the grid. The PV-battery system can be working in either grid-connected or islanded modes by changing the breaker status at the PCC, subject to the condition of the system and the grid, e.g., a serious fault on the AC bus may require opening the breaker to prevent the back-feeding current from the grid. Since PV output power and load demand may change constantly during a day, the power management algorithms for PV-battery system are required to manage the power flow and promptly respond to any change to maintain the balance between power productions and consumptions. Furthermore, both DC bus and AC bus voltages must be stabilized regardless of changes in the system to ensure a reliable power supply.

The minimum required battery size, depends on the critical load that the MG must be capable of feeding when both the solar and wind, are unavailable. In this way, the storage may be oversized. However, in the proposed MG, hydro also supports the critical load, thus the battery size is reduced. Moreover, initial and operational costs, are low and

maintenance requirement is also less. The small hydro power plant in remote regions is recognised as a promising energy source to generate electricity. The small hydro system up to 100 kW rating does not require governor control based turbine prime mover and curtails down the cost of the turbine. The generator used in the small hydro has many variations. Synchronous generator, permanent magnet synchronous generator, synchronous reluctance generator and self-excited induction generator (SEIG), are some of them. However, the most cost effective, efficient, rugged, and easy to use generator in the small hydro system is SEIG. Additionally, the maintenance requirement is also less as compared with its synchronous counterpart. Moreover, SEIG has the drawback that it demands reactive power or magnetising current for producing the desired terminal voltage. Therefore, an excitation capacitor bank provides magnetising current for regulating the terminal voltage of the generator. The hydro-based generating system operates in almost constant power mode so that if the load changes, the frequency, and voltage also changes from their reference values. Therefore, voltage and frequency in the standalone SEIG based hydro system are maintained with the help of an electronic load controller.

In this system, PV-battery-hydro based MG is designed for low voltage, which supplies power to small pockets of customers. The proposed MG consists of two energy sources namely hydro and PV with BES. The hydro-based MG adds stiffness and inertia to the system voltage and also increases the reliability of the MG as compared with the wind based MG. An integration of BES eliminates the need for a dump load and adds to the functionality of the MG. This BES is controlled by a bidirectional converter, which reduces the capacity of storage and utilises the battery effectively. Moreover, BES maintains the continuity of the supply in varying load conditions. The generation of stable, maximum and continuous energy from the PV array is achieved through incremental conductance (INC) maximum power point tracking (MPPT) technique. Additionally, some ancillary services are achieved like current harmonics mitigation, voltage harmonics reduction and reactive power support at the point of common interconnection (PCI). The VSC switching is based on the synchronous reference frame (SRF) theory. Therefore, the proposed standalone PV hydro based MG is highly suitable to serve the remote places where electrification is either not yet done or the cost of the electrification is costly. The proposed MG has the following distinctive features:

1. In the proposed MG, the hydro generator runs at almost constant power, therefore, the sudden load change causes the frequency and generated a voltage at PCI to vary. One way of regulating the voltage and frequency is by controlling the water inlet to the hydro through the

mechanical controller. However, due to the mechanical devices involved, the dynamic response of the controller is not very fast. Therefore, the mechanical speed regulator is not suitable for sudden changing loads. Therefore, in this proposed MG, the storage battery with VSC, is used to regulate the frequency of the system.

2. During the period of a load change, the controller estimates the load power demand and total generated power. If the load demand is more than the generated power, the controller draws there maining power from the battery to balance the power demand. Similarly, for light load condition, the battery takes the extra power to maintain the frequency of the system.

3. The proposed MG is also suitable to feed the non-linear load and the harmonic currents required by the non-linear load are supplied by the VSC. Therefore, the hydro generator does not supply the harmonic currents and voltage at PCI is of good quality.

4. The proposed MG mitigates the negative impacts of solar PV array caused by the intermittent nature of the solar irradiance. Due to this intermittency, the power generated by the solar PV array changes continuously. Therefore, the storage battery absorbs power fluctuations and maintains the frequency of the MG.

5. In the proposed MG, the battery is connected to the DC link of the VSC through BDDC, rather than connecting the battery directly at DC link. The advantage of not connecting the battery directly at DC-link reduces the voltage rating of the battery. Moreover, the battery is not directly exposed to the DC link ripple mostly dominant second harmonic. In this proposed topology, the filter of the BDDC smoothens the charging current, thereby, increasing the battery life.

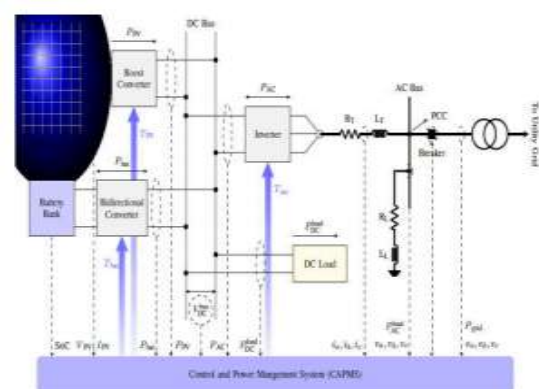


Fig. 1. The proposed control and power management system (CAPMS) for PV-battery-based hybrid microgrids.

## 2. Structure and design of proposed MG

The proposed MG consists of two RES namely hydro, solar PV array along with a BES, a boost converter for MPPT

operation and a BDDC for the battery control, as shown in Fig. 1a. A SEIG is used as a hydro generator, which is driven by an unregulated turbine operating in the constant power region. A VSC is connected to the PCI through the coupling inductors. The battery shares the common DC bus of the VSC through the BDDC and solar PV system is also connected to the DC bus of the VSC through the boost converter. Moreover, the ripple filter, linear and non-linear loads are connected to the PCI. The hardware implementation of the proposed MG is done using the digital processor (dSPACE-1103). The inputs of the digital processor are PCI voltages, load currents, source currents, battery current, sensed DC bus voltage, solar PV voltage, and current. However, these parameters are sensed using the Hall-effect voltage and current sensors. After this, the digital processor reads these sensed data via analog to digital converter (ADC) and processes according to the SRF based control algorithm and generates the switching pulses for the VSC.

**2.1 Design of PV boost converter**

The solar PV array is made of modules, which are connected in series and parallel. In an experimental prototype, a solar PV array rating is considered as 2.48 kW. The solar PV maximum power is extracted in two stages. The first stage is to harness the maximum available from the solar PV array using a boost converter and the second stage is to deliver the maximum harnessed power to the load and the battery. The input voltage of a boost converter is the maximum power point (MPP) voltage of the PV array, which is considered as 307 V. The inductor ( $L_b$ ) of the boost converter is designed for a duty cycle estimated as

$$D = (V_{dc} - V_{pv}) / V_{dc} = (360 - 307) / 360 = 0.147. \quad (1)$$

The designed value of a boost inductor is given as [8]

$$L_b = \frac{V_{mp} \times D}{\Delta i_p \times f_s} = \frac{307 \times 0.15}{0.1 \times 8 \times 20 \times 10^3} = 2.87 \text{ mH} \cong 3 \text{ mH}, \quad (2)$$

where ripple current is equal to 10% of the solar PV current at MPP and  $f_s$  is switching frequency, which is considered as 20 kHz.

**2.2 Design of DC bus capacitor and coupling inductors of VSC**

The minimum DC bus voltage for power transfer should be at least equal to 1.1 times the peak of line voltage, i.e.  $V_{dc} = 1.1 \times V_{sab} \times 2 = 230 \times 2 \times 1.1 = 358 \text{ V}$ . Therefore, a DC bus

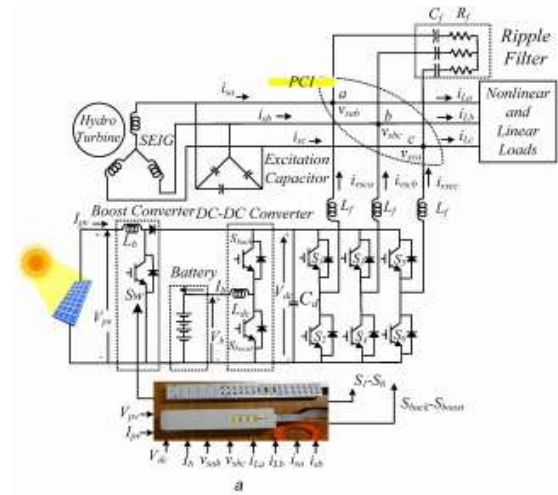


**Fig. 1 Microgrid Topology and MPPT Control**  
(a) Proposed PV-battery-hydro MG, (b) INC based MPP algorithm

capacitor is calculated for DC bus voltage of 360 V and it is given as

$$C_d = \frac{P_{dc} / V_{dc}}{2 \times \omega \times \Delta V_{dc}} = \frac{2485 / 360}{2 \times 314 \times 0.015 \times 360} = 2854.61 \mu\text{F} \cong 3000 \mu\text{F}. \quad (3)$$

The interfacing inductor is designed for elimination of high frequency switching harmonics from the VSC current. The coupling inductor is designed as [18]

$$L_r = \frac{m \times V_{dc}}{6 \times f_s \times h \times \Delta i_c} = \frac{360}{6 \times 10 \times 10^3 \times 1.2 \times 11 \times 0.10} = 4.5 \text{ mH} \cong 5 \text{ mH}. \quad (4)$$

where  $f_s$  is the switching frequency and it is considered as 10 kHz.  $\Delta i_c$  is the ripple current and it is considered as 10% of fundamental supply current.  $m$  and  $h$  are the constant values, which are considered as 1 and 1.2, respectively

**2.3 Design of bidirectional converter**

The bidirectional DC-DC inductor (BDDC), which connects the battery to the DC bus, is designed to operate as a buck converter while charging the battery and operates as a boost

converter in the battery discharging mode. This inductor of the BES is designed as,

For buck mode operation of the bidirectional converter, filter inductor of the battery is designed as duty cycle  $(D) = V_b / V_{dc} = 240/360 = 0.66$ , and an inductor,  $L_{dc}$  is as

$$L_{dc} = \frac{D(V_{dc} - V_b)}{f_s \Delta I_L} = \frac{0.66 \times (360 - 240)}{20 \times 10^3 \times 5 \times 0.2} = 3.96 \text{ mH} \cong 4 \text{ mH}, \quad (5)$$

where  $V_b$  is the battery voltage and it is 240 V,  $V_{dc}$  is the DC-link voltage and it is considered as 360 V.  $\Delta I_L$  is the ripple current and it is considered as 20% of charging current.  $f_s$  is the switching frequency and its value is 20 kHz.

For boost mode operation of bidirectional converter, the filter inductor of the battery is designed as duty cycle  $(D) = (V_{dc} - V_b) / V_b = (360 - 240)/360 = 0.33$

$$L_{dc} = \frac{V_b D}{f_s \Delta I_L} = \frac{0.33 \times 240}{20 \times 10^3 \times 5 \times 0.2} = 3.96 \text{ mH} \cong 4 \text{ mH}, \quad (6)$$

where  $V_{dc}$  is the DC link voltage and it is 360 V.  $V_b$  is the battery voltage and it is 240 V.  $\Delta I_L$  is the ripple current and it is considered as 20% of discharging current. Therefore, the filter inductor of the BES is considered as 4 mH.

## 2.4 Design of battery and ripple filter

Based on the total capacity of the hydro and solar PV array, the energy storage system capacity is selected. In case, the load is isolated from the MG, the battery should be able to take the whole generated power of the hydro and solar PV array. Moreover, in this extreme operating condition, the battery should regulate the frequency and voltage of the MG. Hence, the battery rating is selected as 240 V, 14 Ah. The ripple filter is designed to suppress the high-frequency noise caused by the switching the VSC. The ripple filter is a low pass filter and it is the series combination of the capacitor and resistance and their values, are selected as 10  $\mu\text{F}$  and 5  $\Omega$ . The other parameters of the MG are given in the Appendix.

## 3. THE PROPOSED CONTROL AND POWER MANAGEMENT SYSTEM

The proposed CAPMS is a centralized power management system consisting of a supervisory module that monitors the required realtime parameters (dashed lines in Fig. 1) from the PV battery system and multiple controllers for each of the power converters. According to the situation of the monitored parameters, CAPMS decides the scenarios and select specific control schemes to be applied to the converters to ensure a reliably power environment.

Although the proposed CAPMS is designed based on the PV-battery system configuration shown in Fig. 1, for other configurations, such as systems with decentralized inverters or multiple battery banks, similar approach may be applicable with proper modifications. Detailed schemes of the CAPMS, taking into account both grid connected and islanded modes, are depicted in Fig. 2, which indicates the possible operating scenarios of the PV-battery microgrid and how CAPMS responds to control and balance the system.

As presented in the flowcharts, the PV-battery system, which connects to the grid via a circuit breaker, can operate either in islanded or gridconnected mode, depending on the conditions and plans of both the microgrid and main grid. Firstly, the CAPMS monitors the status of circuit breaker and determines different voltage and power control schemes to be applied to corresponding converters or inverter. In particular, in grid connected mode, the inverter controls the DC bus voltage ( $V_{bus DC}$ ) and reactive power (QAC) that is exchanged with the AC side; the PV converter controls the power output of the PV array (PPV); and the battery converter manages the charging or discharging of the battery bank. In islanded mode, where the breaker is open, CAPMS has to ensure the reliability of electric power supplied to the loads, i.e., DC and AC bus voltages and AC frequency have to be maintained around set points within acceptable limits, to prevent damaging the loads during transitions. Therefore, upon transferring from grid-connected to islanded mode, the inverter switches to regulate the AC bus voltage ( $v_a$ ,  $v_b$ , and  $v_c$ ) and frequency ( $f$ ), while  $V_{bus DC}$  is regulated by the battery converter. Secondly, state of charge (SoC) of the battery bank is always monitored in both modes. Therefore, CAPMS is aware of the available energy storage that can be used in the battery. The upper and lower limits of the SoC (SoC upper limit and SoC lower limit) are set up to make sure the battery is not over-charged or discharged and to increase its cycle life [27]. Depending on the PV output power, SoC and power limit of the battery, DC and AC loads, and the grid demand, CAPMS decides the operation modes of the PV array (MPPT or power-reference mode) and the battery (charging or discharge mode) and provides proper reference values to the controllers, if applicable. Therefore, power flows in the hybrid microgrid are always balanced. The power management criteria are based on

$$\text{Grid-connected: } P_{PV} + P_{bat} = P_{DC}^{load} + P_{AC}^{load} + P_{grid}, \quad (1)$$

$$\text{Islanded: } P_{PV} + P_{bat} = P_{DC}^{load} + P_{AC}^{load}, \quad (2)$$

where PPV is the output power of the PV array, Pbat is the power flows in the battery converter ( $P_{bat} < 0$  in charging mode and  $P_{bat} > 0$  in discharging mode), Pload DC and Pload AC are DC and AC loads, respectively, and Pgrid generally represents the power exchanging between the

main grid and the microgrid through the breaker ( $P_{grid} < 0$  when receiving power and  $P_{grid} > 0$  when sending power).

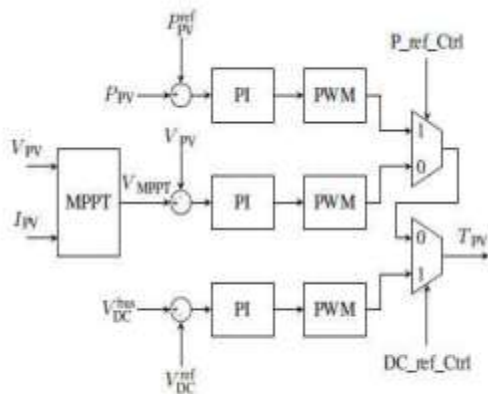


Fig. 6. PV array controller.

Note that the power demand from the main grid is denoted as  $P_{demand}$  grid (Fig. 9), which might be obtained by forecasting data. Before switching from islanded to grid-connected mode, CAPMS will synchronize the AC voltages at the PCC of the microgrid to follow the grid-side voltages to ensure a smooth transition with well-balanced power and regulated voltages, CAPMS ensures an uninterrupted power on both DC and AC buses and allows loads to plug and play in the PV-battery system, regardless of disturbances from switching operating modes. Additionally, since the DC bus voltage is controlled, as long as voltage level matches, DC loads will be able to connect to the DC bus without additional converters. When necessary, the PV-battery system can also provide reactive power to the grid. Detailed controlling schemes for each part of the system will be elaborated in the next section.

### 3.1.CONTROLLER DESIGN OF THE CAPMS

#### A. PV Array Controller

The PV array converts solar energy into DC power, and is connected to the DC bus via a boost DC/DC converter. However, due to nonlinear characteristics of PV panels and the stochastic fluctuations of solar irradiance, there is always a maximum power point (MPP) for every specific operating situation of a PV array. Therefore, maximum power point tracking (MPPT) algorithms are typically implemented in PV system to extract the maximum power a PV array can provide [28]. The proposed CAPMS employs one of the most popular methods, the Incremental Conductance MPPT, which provides a reference voltage  $V_{MPPT}$  that the PV array will track to produce the maximum power under various operation conditions (different combinations of irradiance and temperature). There are three possible control schemes for the PV array: MPPT control, power reference control, and DC bus voltage control, depending on the

situation of the PV-battery system. For example, in islanded mode, when PMPPT PV is greater than the total load demand (DC and AC), and the battery is fully charged or the charging rate  $P_{bat}$  reaches its upper limit, the CAPMS will generate control commands  $P_{ref\_Ctrl} = 1$  and  $DC_{ref\_Ctrl} = 0$  to set the PV array to work in power-reference control mode by sending PWM streams,  $T_{PV}$ , to the DC/DC converter accordingly. In this case, to balance the power flows, CAPMS will decide proper power references for the PV array,  $P_{ref\_PV}$ , according to the value of which the operating voltage of the PV array,  $V_{PV}$ , will be moving between its  $V_{MPPT}$  and the open-circuit voltage,  $V_{OC}$ .

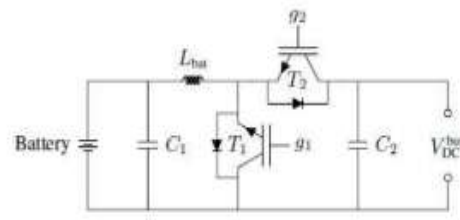


Fig. 7. Bidirectional DC/DC converter for the battery bank.

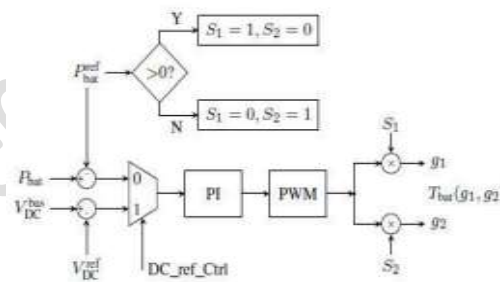


Fig. 8. Battery charging/discharging controller.

Since the DC bus voltage is regulated by the battery converter in this situation, there will be a stable voltage at the DC bus in spite of the fluctuations in  $V_{PV}$ . In MPPT mode ( $P_{ref\_Ctrl} = 0$  and  $DC_{ref\_Ctrl} = 0$ ), real-time PV current,  $I_{PV}$ , and  $V_{PV}$  are measured and sent to the MPPT module, which then provides  $V_{MPPT}$  as the voltage reference for the PV array. Additionally, in islanded mode, when the battery is not available, e.g., due to faults, the PV converter has to switch to control the DC bus voltage to ensure a stable power supply to the loads on the DC bus ( $P_{ref\_Ctrl} = 0$  and  $DC_{ref\_Ctrl} = 1$ ). Fig. 6 illustrates the controller for these three modes. Note that the situation where both  $P_{ref\_Ctrl} = 1$  and  $DC_{ref\_Ctrl} = 1$  is not applicable.

#### B. Battery Controller

As an energy buffer, battery bank is necessary in PV systems for power balancing. The battery bank of this system is connected to the DC bus and is controlled by a bidirectional DC/DC converter (Fig. 7) which includes two switches,  $T_1$  and  $T_2$ , that control the charging/discharging

process. Fig. 8 explains the detailed control process. In grid-connected mode, with the command DC ref Ctrl = 0, the converter controls the power flow (Pbat) in or out of the battery, where in discharging mode  $P_{bat} > 0$ , and in charging mode  $P_{bat} < 0$ . The final output of the battery controller is a two-dimensional switching signal Tbat (g1; g2). In Islanded mode, the control command DC ref Ctrl is set to “1” by the CAPMS, which switches the converter to work in voltage reference mode. The output voltage of converter, which is also the DC bus voltage, is regulated to follow the reference so that the DC load voltage is stabilized. The CAPMS monitors the SoC of the battery and enforces its upper and lower limits (SoCupper limit = 90% and SoClower limit = 10% in this study) in order to increase the life cycle. Note that the selections of the SoC limits do not affect the performance of the controller.

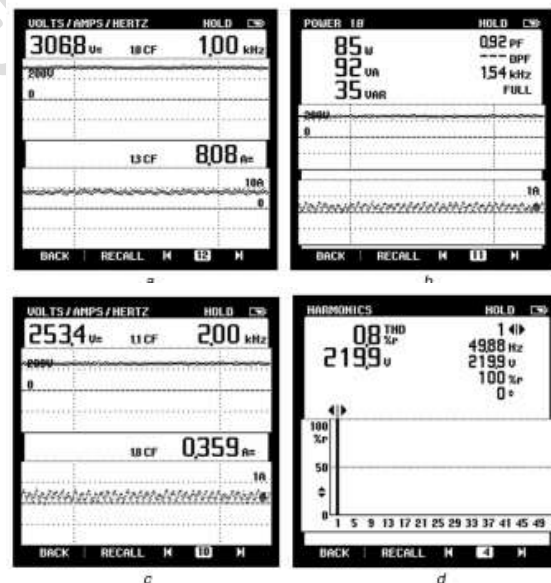
### C. Inverter Controller

A three-phase inverter is used to convert DC to AC power, interfacing the DC and AC sides. Similar to the converters discussed above, the control scheme of inverter depends on the operating (grid-connected or islanded) mode of the system. As is illustrated in Fig. 1 and 6, in grid-connected mode, a phase locked loop (PLL block) is employed to extract  $\omega$ , angle of the phase-A voltage after the breaker (ea). In islanded mode,  $\omega$  is generated locally, which periodical ramp signal is varying from 0 to  $2\pi$  with frequency f. It is used to decompose the three-phase AC bus voltages (va; vb and vc) and the inverter output currents (ia; ib and ic) into d-q frame variables  $V_d$  and  $V_q$ , and  $I_d$  and  $I_q$  by Park transformation, respectively, for control purposes. Depending on the operating mode, the controller selects different sets of variables to be controlled. Under islanded mode, CAPMS sets the signal “Islanded” to 1, forcing the converter to regulate the AC bus voltage  $V_d$  and  $V_q$ . Frequency of the AC bus voltages (f) is set to 60 Hz in a open loop manner. Before closing the breaker and reconnecting the PV-battery system to the grid, the AC bus voltage must be synchronized with the grid. During islanded mode, the signal “Sync” is set to 0 so that CAPMS has full control of the AC bus voltage by adjusting the references,  $V_{ref d}$  and  $V_{ref q}$ . However, to ensure a smooth transition upon switching to grid connected mode, “Sync” will be set to 1 to synchronize the AC bus and grid side voltages right before closing the breaker. To this end,  $\omega$  will be synchronized to follow the output angle of PLL, and the AC voltages after the breaker in d-q frame,  $E_d$  and  $E_q$ , will be chosen as the references for  $V_d$  and  $V_q$ .

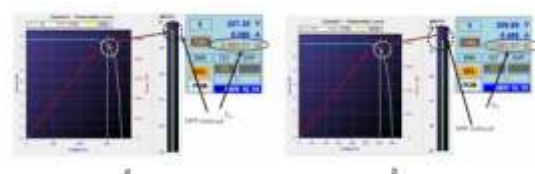
## 4. RESULTS AND DISCUSSION

The proposed MG is implemented for a 3.7 kW hydro based induction generator, PV array simulator and BES. The excitation capacitor of the SEIG has been selected

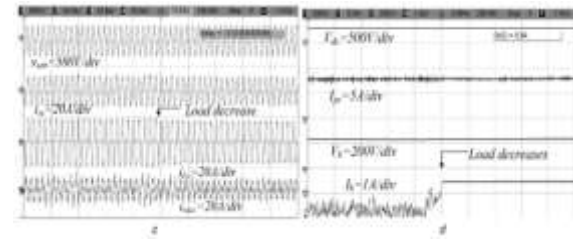
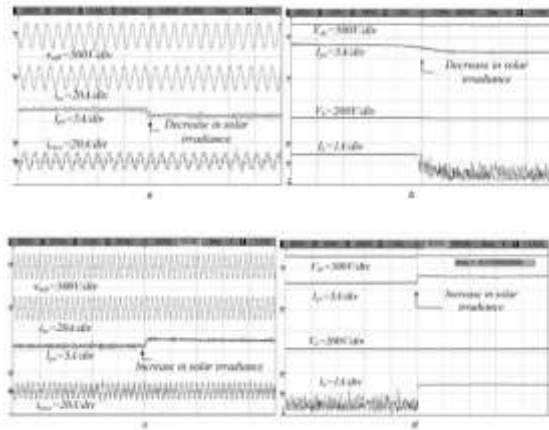
by using the per-phase equivalent model of SEIG as per the procedure. The per phase excitation capacitor of 3.7 kW, 230 V, 50 Hz, induction machine is selected as 80  $\mu$ F/phase. Moreover, these capacitors are connected in delta configuration and it is connected to the generator terminals to maintain the rated voltage. A variable frequency drive controlled induction motor is used for emulating the hydro prime mover. A non-linear load is realised by using the diode bridge rectifier with the R-L load. Six Hall-effect current sensors are used for sensing the source currents (isa and isb), load currents (iLa and iLb), solar PV current (I<sub>pv</sub>) and battery current (I<sub>b</sub>). Four Hall-Effect voltage sensors are used for sensing the common point voltages (vsab and vsbc), PV voltage (V<sub>pv</sub>) and the DC bus voltage of the converter (V<sub>dc</sub>). A PV array simulator (TerraSAS PV) is used to realise a 2.48 kW solar PV, whose maximum voltage (V<sub>mpp</sub>) and current (I<sub>mpp</sub>) rating are 307.0 V and 8.0 A, respectively. The control algorithm of the VSC and a bidirectional converter for voltage, frequency and power management, are implemented on a digital controller (dSPACE-1103). The system voltage and frequency regulation are achieved by PI controllers. The PI controllers of the proposed MG are tuned using the Ziegler Nichols step response technique .



Steady-state performance of PV-battery-hydro system under non-linear load (a)  $V_{pv}$  and  $I_{pv}$ , (b)  $P_b$ , (c)  $V_b$  and  $I_b$ , (d) Harmonic spectra of vsab



MPPT performance (a) at 1000 W/m<sup>2</sup> , (b) at 790 W/m<sup>2</sup>



#### 4.2 Dynamic performance of PV-battery-hydro based MG under change in solar irradiance

The dynamic performance of the PV-battery-hydro based MG under solar irradiance disturbance is shown in Figs.a–d and 6b. In Figs.a–d, the dynamic behaviour of the PCI voltage ( $v_{sab}$ ), source current ( $i_{sc}$ ), load current ( $i_{Lc}$ ), VSC current ( $i_{vscc}$ ), DC-link voltage ( $V_{dc}$ ), solar PV array current ( $I_{pv}$ ), battery voltage ( $V_b$ ) and battery current ( $I_b$ ), is exhibited. Despite the change in solar PV irradiance from 1000 to 790 W/m<sup>2</sup>, MPP is achieved as shown in Fig. b. A reduction in solar PV irradiance, causes the change in solar generated power and consequently, the change in battery operating mode from charging to discharging mode, to meet the load demand as shown in Fig. b. The other system parameters remain unaffected and the system remains stable. Similarly, an increase in solar PV irradiance, increases the power generated by the solar PV array. To manage the increased power, the battery changes the operating from discharging to charging as shown in Figs. 7c–d. The DC-link voltage remains unaffected under the solar irradiance disturbances.

#### 4.3 Dynamic performance of PV-battery-hydro based MG under load perturbation

The dynamic performance of PV-battery-hydro based MG under varying load conditions. Figs.a–d show the transient behaviour of the PCI voltage ( $v_{sab}$ ), source current ( $i_{sc}$ ), load current ( $i_{Lc}$ ), VSC current ( $i_{vscc}$ ), DC-link ( $V_{dc}$ ), solar array current ( $I_{pv}$ ), battery voltage ( $V_b$ ) and battery current ( $I_b$ ). When the load is increased, load demand exceeds the hydro generated power, since SEIG operates in constant power mode. In this condition, the solar power is diverted to meet the load demand and the battery starts discharging as shown in Figs.a and b. Similar is the condition for a decrease in load demand and the battery comes into charging mode, which is depicted in Figs.c and d.

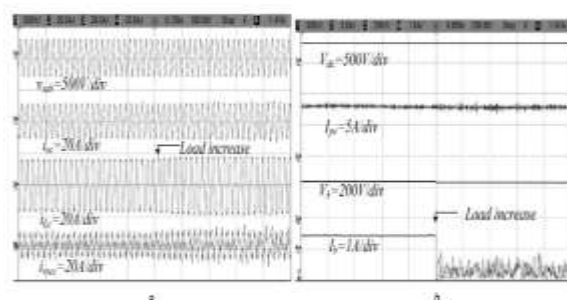
### 5. CONCLUSIONS

In the proposed MG, an integration of hydro with the battery, compensates the intermittent nature of PV array. The proposed system uses the hydro, solar PV and battery energy to feed the voltage ( $V_{dc}$ ), solar array current ( $I_{pv}$ ), battery voltage ( $V_b$ ) and battery current ( $I_b$ ). When the load is increased, the load demand exceeds the hydro

Dynamic performance of PV-battery-hydro based MG following by solar irradiance change (a)  $v_{sab}$ ,  $i_{sc}$ ,  $i_{Lc}$  and  $i_{vscc}$ , (b)  $V_{dc}$ ,  $I_{pv}$ ,  $V_b$  and  $I_b$ , (c)  $v_{sab}$ ,  $i_{sa}$ ,  $i_{La}$  and  $i_{vsca}$ , (d)  $V_{dc}$ ,  $I_{pv}$ ,  $V_b$  and  $I_b$

#### 4.1 Steady-state performance of PV-battery-hydro based MG under non-linear load

The current drawn by the non-linear load contains the harmonics and in the proposed MG, the hydro generated source currents are sinusoidal even when the load currents are non-sinusoidal as shown in Figs.a–d. The load is fed through two energy sources, one is hydro and second is PV array as shown in Figs. a–d. In the proposed MG, the MPPT algorithm harnesses the maximum available power from the solar PV array and the performance of the MPPT algorithm of the solar PV array simulator in the experimental prototype is shown in Fig. a. Solar PV generated power, voltage, and current under maximum power condition and also battery voltage, current and power are shown in Fig. d and a–c. From Fig.d, it is seen that the solar PV generated power is 2.48 kW, which is distributed into three parts (i) supplying the remaining power required by the load, (ii) storing the surplus power in the battery, and (iii) compensating losses of the system. The harmonic spectra of PCI line voltages, source current and load current, are shown in Figs. 3b, d, and 5d. The source current is sinusoidal and its total harmonic distortion (THD) is 4.1% and source voltage THD is 0.8%, which are well within an IEEE-519 standard. However, the load current THD is obtained as 22.3%.



generated power, since SEIG operates in constant power mode condition. This system has the capability to adjust the dynamical power sharing among the different RES depending on the availability of renewable energy and load demand. A bidirectional converter controller has been successful to maintain DC-link voltage and the battery charging and discharging currents. Experimental results have validated the design and control of the proposed system and the feasibility of it for rural area electrification.

## REFERENCES

[1] T. A. Nguyen, X. Qiu, J. D. G. II, M. L. Crow, and A. C. Elmore, "Performance characterization for photovoltaic-vanadium redox battery microgrid systems," *IEEE Trans. Sustain. Energy*, vol. 5, no. 4, pp. 1379–1388, Oct 2014.

[2] S. Kolesnik and A. Kuperman, "On the equivalence of major variable-step-size MPPT algorithms," *IEEE J. Photovolt.*, vol. 6, no. 2, pp. 590–594, March 2016.

[3] H. A. Sher, A. F. Murtaza, A. Noman, K. E. Addoweesh, K. Al-Haddad, and M. Chiaberge, "A new sensorless hybrid MPPT algorithm based on fractional short-circuit current measurement and P&O MPPT," *IEEE Trans. Sustain. Energy*, vol. 6, no. 4, pp. 1426–1434, Oct 2015.

[4] Y. Riffonneau, S. Bacha, F. Barruel, and S. Ploix, "Optimal power flow management for grid connected PV systems with batteries," *IEEE Trans. Sustain. Energy*, vol. 2, no. 3, pp. 309–320, July 2011.

[5] H. Kim, B. Parkhideh, T. D. Bongers, and H. Gao, "Reconfigurable solar converter: A single-stage power conversion PV-battery system," *IEEE Trans. Power Electron.*, vol. 28, no. 8, pp. 3788–3797, Aug 2013.

[6] Z. Yi and A. H. Etemadi, "A novel detection algorithm for line-to-line faults in photovoltaic (PV) arrays based on support vector machine (SVM)," in *2016 IEEE Power and Energy Society General Meeting (PESGM)*, July 2016, pp. 1–4.

[7] Ellabban, O., Abu-Rub, H., Blaabjerg, F.: 'Renewable energy resources: current status, future prospects and technology', *Renew. Sustain. Energy Rev.*, 2014, 39, pp. 748–764.

[8] Bull, S.R.: 'Renewable energy today and tomorrow', *Proc. IEEE*, 2001, 89, (8), pp. 1216–1226

[9] Malik, S.M., Ai, X., Sun, Y., et al.: 'Voltage and frequency control strategies of hybrid AC/DC microgrid: a review', *IET Renew. Power Gener.*, 2017, 11, (2), pp. 303–313.

[10] Kusakana, K.: 'Optimal scheduled power flow for distributed photovoltaic/ wind/diesel generators with battery storage system', *IET Renew. Power Gener.*, 2015, 9, (8), pp. 916–924.

## AUTHOR'S PROFILE:

[1]. **B.MANI** Pursuing her Masters Degree in Department of EEE from Kakinada Institute Of Technological Sciences (Kits), Ramachandrapuram.



Electronics.

[2]. **PUVVULA HEMANTH PRITHVI**, Completed his B.Tech and M.Tech Degrees from Aditya Engineering College, Surampalem. Presently he is working as Assistant Professor in Department of EEE, KITS College, Ramachandrapuram. His Interested Area is Power